Overexpression of chromatin remodeling and tyrosine kinase genes in iAMP21-positive acute lymphoblastic leukemia

Ingegerd Ivanov Öfverholm, Vasilios Zachariadis, Fulya Taylan, Yanara Marincevic-Zuniga, Anh Nhi Tran, Leonie Saft, Daniel Nilsson, Ann-Christine Syvänen, Gudmar Lönnerholm, Arja Harila-Saari, Magnus Nordenskjöld, Mats Heyman, Ann Nordgren, Jessica Nordlund & Gisela Barbany

Taylor & Francis
Taylor & Francis Group

ORIGINAL ARTICLE

OPEN ACCESS | Check for updates

Overexpression of chromatin remodeling and tyrosine kinase genes in iAMP21-positive acute lymphoblastic leukemia

Ingegerd Ivanov Öfverholm[a,b] (ID), Vasilios Zachariadis[c] (ID), Fulya Taylan[a] (ID), Yanara Marincevic-Zuniga[d] (ID), Anh Nhi Tran[a,b], Leonie Saft[e], Daniel Nilsson[a,b,f] (ID), Ann-Christine Syvänen[d], Gudmar Lönnerholm[g], Arja Harila-Saari[h], Magnus Nordenskjöld[a,b] (ID), Mats Heyman[h], Ann Nordgren[a,b] (ID), Jessica Nordlund[d] (ID) and Gisela Barbany[a,b]

[a]Department of Molecular Medicine and Surgery and Center for Molecular Medicine, Karolinska Institutet, Stockholm, Sweden; [b]Department of Clinical Genetics, Karolinska University Hospital, Stockholm, Sweden; [c]Department of Oncology-Pathology, Karolinska Institutet, Stockholm, Sweden; [d]Department of Medical Sciences, Molecular Medicine and Science for Life Laboratory, Uppsala University, Uppsala, Sweden; [e]Department of Pathology, Karolinska University Hospital, Stockholm, Sweden; [f]Science for Life Laboratory, Karolinska Institutet Science Park, Stockholm, Sweden; [g]Department of Women's and Children's Health, Uppsala University, Uppsala, Sweden; [h]Department of Women's and Children's Health, Karolinska Institutet, Karolinska University Hospital Solna, Stockholm, Sweden

ABSTRACT

Intrachromosomal amplification of chromosome 21 (iAMP21) is a cytogenetic subtype associated with relapse and poor prognosis in pediatric B-cell precursor acute lymphoblastic leukemia (BCP ALL). The biology behind the high relapse risk is unknown and the aim of this study was to further characterize the genomic and transcriptional landscape of iAMP21. Using DNA arrays and sequencing, we could identify rearrangements and aberrations characteristic for iAMP21. RNA sequencing revealed that only half of the genes in the minimal region of amplification (20/45) were differentially expressed in iAMP21. Among them were the top overexpressed genes ($p < 0.001$) in iAMP21 vs. BCP ALL without iAMP21 and three candidate genes could be identified, the tyrosine kinase gene DYRK1A and chromatin remodeling genes CHAF1B and SON. While overexpression of DYRK1A and CHAF1B is associated with poor prognosis in malignant diseases including myeloid leukemia, this is the first study to show significant correlation with iAMP21-positive ALL.

Introduction

In childhood acute lymphoblastic leukemia (ALL), detection of known cytogenetic markers at diagnosis is important for risk stratification and guides the choice of treatment intensity. In the Nordic Society of Pediatric Hematology and Oncology (NOPHO) treatment protocol, six genetic markers are used to upgrade risk stratification of patients because of association with risk for relapse and treatment resistance [1]. Intrachromosomal amplification of chromosome 21 (iAMP21) is an intermediate risk marker present in 2% of pediatric BCP ALL; the subtype is associated with high age, low white blood cell count [2,3] and a high relapse rate if treated according to standard risk protocols [4–6]. A previous study demonstrated that iAMP21 patients treated according to high risk protocols had a reduced risk of relapse [7], however, data from the NOPHO 2008 protocol show that iAMP21 is associated with dismal prognosis despite intensive treatment [8].

The iAMP21 subtype has been investigated extensively at the genomic level, with studies describing the composition of the amplified chromosome and the mechanisms of formation [9–13]. Others and we have shown that iAMP21 is primary event [11] associated with specific copy number alterations (CNAs) [14–16], genomic fusions [7,11] and mutations in RAS pathway genes [17]. However, the only genetic alteration recurrent in all iAMP21 cases is an amplification of a 5 Mb region on chromosome 21q [11] and although the leukemia promoting mechanism in iAMP21 is thought to originate from this region, no causative genes have thus far been identified in the region.

CONTACT Ingegerd Ivanov Öfverholm ✉ ingegerd.ofverholm@ki.se 🖳 Department of Molecular Medicine and Surgery, Karolinska Institutet, Clinical Genetics Section L5:03, Karolinska University Hospital Solna, SE-171 76 Stockholm, Sweden

ⓘ Supplemental data for this article can be accessed here.

In this study, we use an integrated approach to investigate the structure and transcriptional effects of the iAMP21 rearrangement, and we show that the amplification of chromosome 21 affects several potential oncogenes involved in cell cycle regulation and chromatin remodeling.

Patients and methods

Patients and clinical data

Diagnostic iAMP21 cases treated according to NOPHO ALL-1992 ($n = 2$), ALL-2000 ($n = 11$) and ALL-2008 ($n = 2$) protocols with samples available in the NOPHO biobank in Uppsala and sample collection at Karolinska University hospital ($n = 15$) were included together with relapse samples from two patients. A majority of cases were diagnosed by routine fluorescence *in situ* hybridization (FISH) and defined by ≥ 5 signals from the *RUNX1* gene when polysomy 21 had been excluded. Three additional cases were identified through a methylation classifier described by Nordlund et al [18] and retrospectively confirmed by FISH. Clinical data were obtained from the NOPHO registry. Median age at diagnosis was 9 years (range 5–17 years) and median WBC count 5.5×10^9/l (range 1.7–61.5×10^9/l). Clinical and cytogenetic data are summarized in Supplementary Table 1. An additional cohort of 34 BCP ALL cases without iAMP21, i.e. B-other ($n = 2$), t(12;21) ($n = 4$), t(9;20) ($n = 4$), 11q23 rearrangement ($n = 4$), high hyperdiploidy (HeH) ($n = 6$) and dic(9;20) ($n = 14$) [19], was included as a reference cohort. The study was performed in accordance with the declaration of Helsinki and the local ethical board in Stockholm, Sweden, approved the study.

DNA was extracted at the time of diagnosis using QIAgen DNA extraction kits (QIAgen, GmbH, Hilden, Germany). RNA from diagnostic ($n = 14$) and relapse ($n = 2$) bone marrow iAMP21 samples was prepared using the QIAgen All-Prep DNA/RNAMini kit in the scope of the study. The assays performed for each sample are shown in Supplementary Figure 1.

SNP array and copy number analysis

DNA from diagnostic ($n = 12$) and relapse ($n = 1$) bone marrow samples was analyzed with Omni 2.5 M ($n = 9$) or Omni 2.5 M + Exome ($n = 4$) genotyping arrays (Illumina Inc, San Diego, CA, USA) according to the manufacturer's instruction (Illumina.com) to detect CNAs and loss of heterozygosity (LOH). Sample probe intensities were normalized against a panel of internal human controls to produce log2 ratios centered at zero for a diploid sample; log2 ratios were segmented using circular binary segmentation [20]

and segmented copy number (CN) data combined with allele frequencies (BAF) were used to detect allele-specific CNAs using the Tumor Aberration Prediction Suite [21]. Segments of ≥ 10 aberrant probes and spanning ≥ 20kb were included in the analysis. CNAs reported as benign in the Database of Genomic Variants (http://dgv.tcag.ca/dgv/app/home) or in the in-house database for germline CN variants at the department of Clinical Genetics, Karolinska University Hospital, were excluded from further analysis. Annotation and filtering was performed using BEDOPS v2.4.2 [22], R v3.1.0 and visualization was performed using the Integrative Genomics Viewer (IGV) [23].

Mate pair whole genome sequencing (MP-WGS) and data analysis

Mate-pair libraries were prepared from DNA of three diagnostic iAMP21 samples using Nextera Mate Pair Sample Preparation Kit (Illumina Inc, San Diego, CA, USA), according to the manufacturer's instruction for a gel-free preparation of 2 kb effective insert size library. The libraries were sequenced on an Illumina HiSeq 2500 sequencer with an average of 3X mapped coverage; the sequencing and analysis procedure is previously described by Tran et al [24]. Mapped reads were processed and analyzed for intra- and interchromosomal translocations using a sliding window method implemented in TIDDIT (https://github.com/TIDDIT) [25].

RNA sequencing

RNA sample quality was measured using the RNA Nano Assay 6000 on a Bioanalyzer 2100 (Agilent Technologies, Santa Clara, CA, USA); RNA samples with RNA integrity number (RIN) values >7 were included and treated with RiboZero from Epicenter (Epicenter, Madison, WI, USA) to eliminate ribosomal RNA. Strand-specific RNA sequencing libraries were prepared from diagnostic ($n = 12$) RNA samples using ScriptSeq v2 (Epibio.com) and sequenced 50 bp paired-end on Illumina HiSeq 2000/2500, producing $\sim$100 million read pairs/sample. All sequence reads were aligned to the human genome reference build GRCh38 (hg38) using Spliced Transcripts Alignment to Reference (STAR) version 2.5.1b [26] with exon junction support from from Gencode gene annotation version 24. The trimmed mean of M-values normalization method [27] was used for normalization of raw read counts, and voom [28] was used for variance normalization. Genes with a count of ≥ 1 per million mapped reads (CPM), in ≥ 2 samples, were included for further analysis. Gene expression levels were also normalized to fragments per kilobase per million mapped reads (FPKM).

Analysis of differential gene expression was performed using the R/Bioconductor package limma [29]. The iAMP21-positive diagnostic cases were contrasted against the combined average expression of 34 diagnostic BCP ALL cases without iAMP21 [19]. Unsupervised hierarchical clustering was performed using Euclidean distances and complete linkage and significance tested by F test statistic in Limma. Pathway analyses were performed using DAVID (https://david.ncifcrf.gov) and Panther (http://pantherdb.org). Identification of fusion genes was performed using FusionCatcher version 0.99.3c beta (Released Oct 9 2014) against genome reference build GRCh38/hg38 and Gencode gene annotation version 24. RNA from two additional diagnostic samples and two relapse samples with lower RNA amount/quality was prepared using a hybridized-based RNA sequencing method (TruSeq RNA Access, Illumina) and were only included in fusion gene analysis.

Validation of findings

Structural rearrangements were manually inspected in IGV [23,30]. Rearrangement breakpoints detected by mate-pair sequencing were validated using PCR for sample KSALL11; the PCR primers were designed using Primer3Plus [31]. Recurrent fusion transcripts detected by RNA sequencing were validated using RT-PCR and Sanger sequencing to characterize the fusion in cDNA (Supplementary Table 2). The expression of candidate genes was quantified by real time RT-PCR. Briefly, 100 ng of RNA from iAMP21 samples ($n = 10$) and other BCP ALL samples ($n = 19$) were reversed transcribed using the Superscript^{TM} VILO^{TM} synthesis kit (ThermoFisher, Waltham, MA, USA) according to the manufacturer's instructions. Gene expression was quantified with Taqman^{TM} Gene Expression Assays (ThermoFisher). GUS was used as reference gene to control for RNA quality and quantity.

Methylation profiling

Previously published Human DNA Methylation 450k Array (Illumina Inc) data on DNA methylation levels from eight of the diagnostic iAMP21 samples [18,32] were reanalyzed in this study. The iAMP21 samples ($n = 8$) were compared to diagnostic BCP ALL samples without iAMP21 ($n = 665$) from Gene Expression Omnibus under series GSE49031 using the non-parametric Wilcoxon rank-sum test. The p-values were corrected for False Discovery Rate (FDR) due to multiple testing. The mean, standard deviation (SD), and mean methylation difference between the two groups was measured. Minimal

cutoff value for the mean absolute differences in DNA methylation ($\Delta\beta$) was set to $\geq \pm 0.2$ in order to identify CpG sites with large difference between the groups [32].

Results

Genomic structure of chromosome 21 in iAMP21

Copy number (CN) alterations and patterns were investigated in 12 diagnostic and one relapse sample using SNP array. The common region of amplification in our cohort mapped to a 13.2 Mb region on chromosome 21, between position 27,826,425 and 41,053,970 (Figure 1). The CN in the amplified regions ranged from 3 to 8 with an average of 5.5 and most of the samples showed oscillating CN states within the amplified region. The highest CN was found in a region with no genes between position 18,839,526 and 18,862,758 in the relapse sample, where the paired diagnostic sample had a CN of 5. All cases had different centromeric breakpoints, and deletion of the telomeric part was present in eight cases (Figure 1). The relapse sample had retained the same amplification delimiting breakpoints as the diagnostic sample; however, the CN state differed for a few regions. Outside of chromosome 21, recurrent focal deletions were detected in RB1 ($n = 5$), SH2B3 ($n = 5$), ETV6 ($n = 4$), ATP10A ($n = 4$), IKZF1 ($n = 2$) and BTG1 ($n = 2$). Deletions in SH2B3 and RB1 were often homozygous (3/5 and 5/5 respectively) and one case showed LOH of the 12q region involving SH2B3.

Three of the diagnostic cases were further analyzed with mate-pair whole genome sequencing (WGS) to investigate the genomic structure of the amplification. All three cases showed additional structural events in the amplified region; KSALL23 showed one internal rearrangement, whereas KSALL17 and KSALL11 had multiple rearrangements ($n = 12$ respectively) (Figure 2). A majority of rearrangements retained the original strand orientation (20/24) but both cases had a few inverted segments (2 and 3 respectively). Only occasionally, rearrangement breakpoints were flanked by segments with different CN; the large majority of breaks joined segments with identical CN (Figure 2). A few of the detected breakpoints involved genes, e.g. PRDM15, CHAF1B and IFNGR2, but no fusion gene was identified. No interchromosomal rearrangements involving chromosome 21 was detected in any of the samples.

Expression profile of iAMP21

The transcriptional effects of the 21q amplification were investigated using RNA sequencing; 12 iAMP21-positive cases were contrasted to 34 BCP ALL cases without
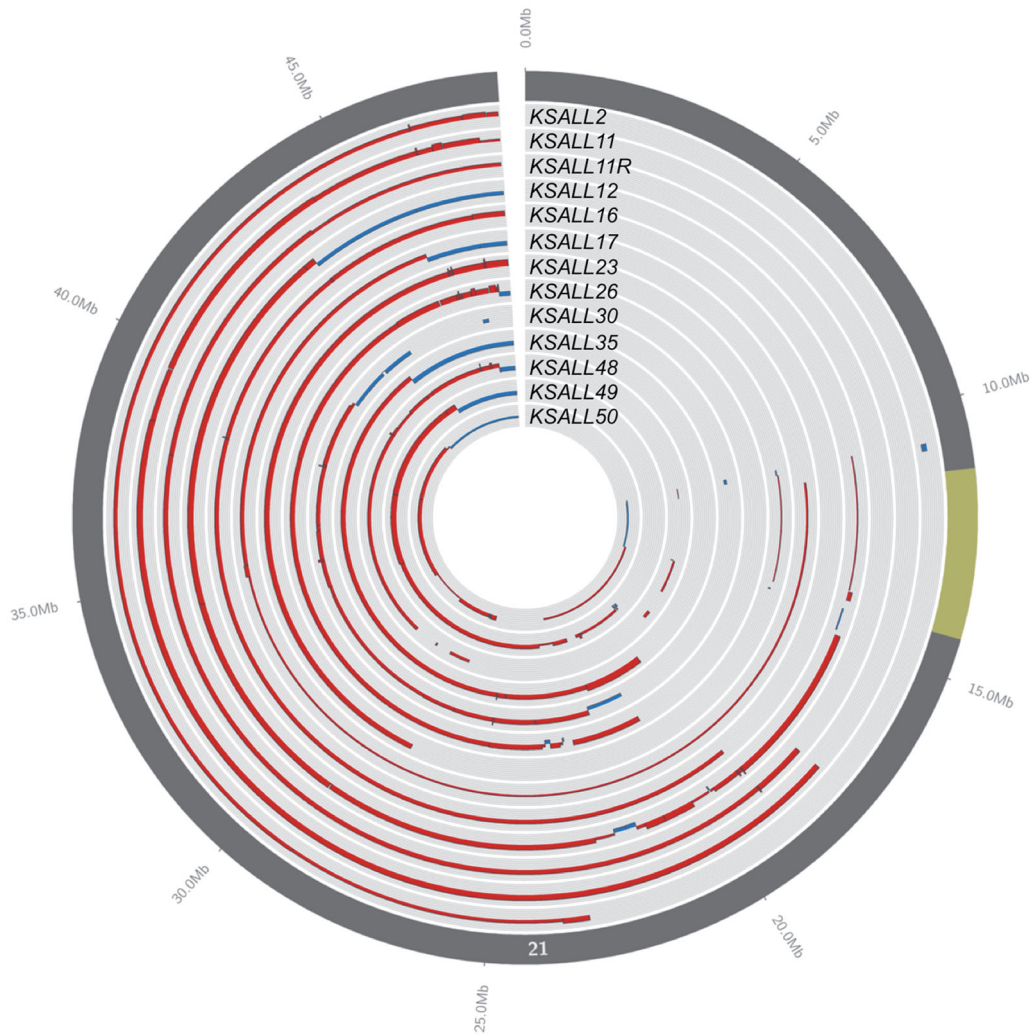
Figure 1. Circos plot showing copy number data on chromosome 21 for iAMP21. White lines separate samples, red and blue lines represent amplifications and deletions respectively, the line thickness corresponds to number of copies gained/lost in each sample. The centromere is highlighted in yellow in the outermost gray circle.

Figure 2. Circos plot of chromosome 21 with intrachromosomal rearrangements detected by mate-pair WGS in three iAMP21 samples. Blue links represent rearrangements retaining the original strand orientation, red links represent inverted rearrangements. Copy number changes are shown with red (amplifications) and blue (deletions) lines in the circos edges.

Figure 3. 2 D Multi-Dimensional Scaling plot of leading log fold changes across the top 1000 genes for each pair of samples. The iAMP21 subtype (green) forms a scattered cluster together with HeH samples (blue). *KSALL50.

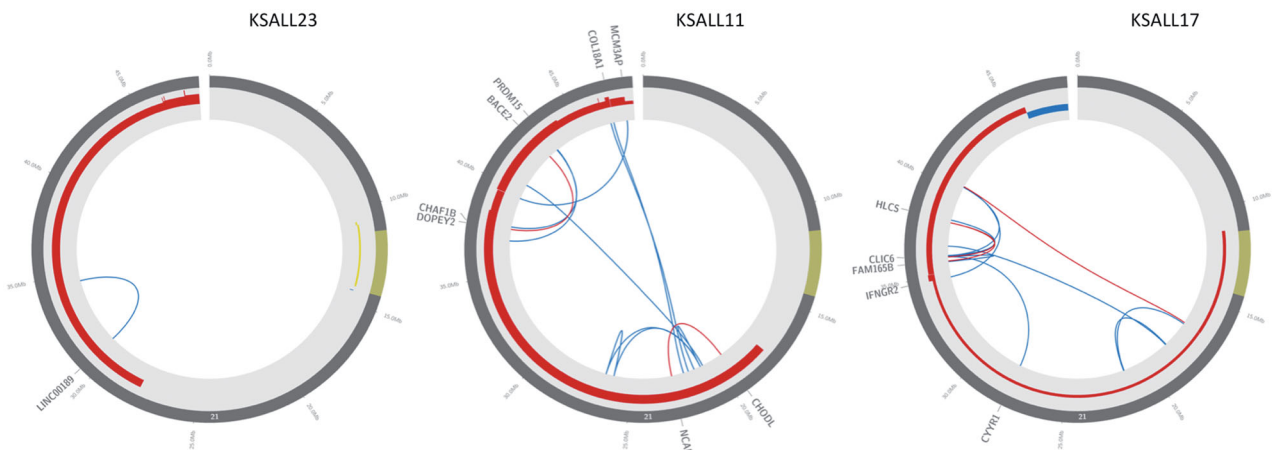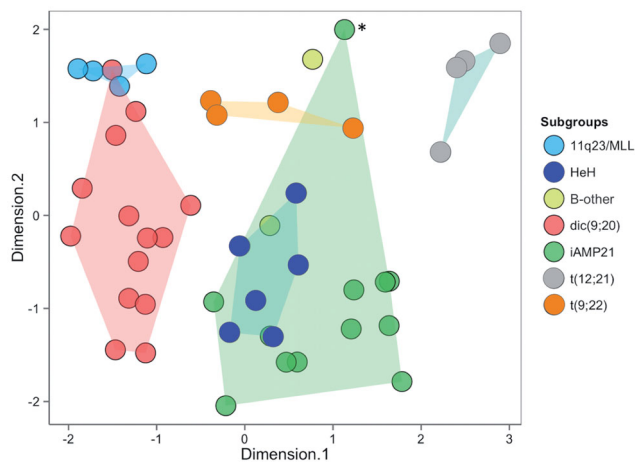iAMP21. Unsupervised 2 D multiple dimensional scaling (MDS) based on the 1000 most variable genes in the cohort showed that the iAMP21 cases formed a scattered cluster, including the HeH cases (Figure 3). KSALL50 did not cluster with the subtype, and further analysis of this case revealed a large amplification on 11q (11q24.3-q25).

Analysis of gene expression levels in iAMP21 vs. BCP ALL without iAMP21 (Log Fold Change >1 and $p \leq 0.05$) showed significantly altered expression of a total of 763 transcripts in iAMP21 (Supplementary Table 3, Supplementary Figure 2). Pathway analysis showed significant enrichment in immune response pathways among the underexpressed genes, while the overexpressed genes were enriched for cellular process pathways, e.g. cell migration, movement and extravasation (Supplementary Table 4(a,b)). Significant enrichment in hematopoietic pathways, including myeloid and lymphoid differentiation, was also observed (Supplementary Table 4(c)) and among the underexpressed genes was a few essential hematopoietic transcription factor genes such as FLI1, RB1 and MEIS1.

The top overexpressed genes ($p < 3.7\mathrm{e}^{-7}$) in iAMP21 were located on chromosome 21, i.e. TTC3, CHAF1B, DYRK1A, HLCS, BRWD1, HMGN1, CRYZL1, SON and TMEM50B (Supplementary Table 5(a)). The leukemia-associated transcription factor ERG was also significantly overexpressed in iAMP21. Analysis of chromosome 21 showed that although iAMP21 and HeH had similar expression patterns, a majority of the top differentially expressed genes in iAMP21 remained significant when iAMP21 was compared with HeH only (Figure 4). Pathway analysis based on the differentially

expressed chromosome 21 genes in iAMP21 did not generate any significant enrichment.

Expression of MRA genes

We subsequently narrowed the analysis to the 5.1 Mb MRA defined by Rand et al. [11], encompassing 45 genes. Less than half of the genes (20/45) were significantly overexpressed in iAMP21 vs. BCP ALL without iAMP21 (Supplementary Table 5(b)) and one third of the overexpressed genes (7/20) were also significantly overexpressed in HeH; the 13 genes that were overexpressed only in iAMP21 are listed in Supplementary Table 5(c). Comparing iAMP21 with HeH only showed that eight MRA genes had significantly higher expression in iAMP21 (Figure 4, Supplementary Table 5(c)); four of these were not significantly overexpressed in HeH vs. BCP ALL without HeH and thus unique for iAMP21, i.e. CHAF1B, SON, DYRK1A and MORC3. Expression levels for the top three genes, CHAF1B, SON and DYRK1A, are shown in a box plot in Figure 5(A). The RNA expression for CHAF1B, SON and DYRK1A was quantified by real-time RT-PCR and the results confirmed high expression in iAMP21 relative to other subtypes (Figure 5(B)). Genes with expression levels that correlated positively or negatively with the expression levels of CHAF1B, SON and DYRK1A in our dataset are listed in Supplementary Table 6(a–c). No correlation between methylation status and expression level of MRA genes could be found (Supplementary Table 7(a,b)).

Fusion transcripts involving chromosome 21

No interchromosomal fusion was detected and the only recurrent fusion involving genes on chromosome 21 was a fusion-inversion of RUNX1-DYRK1A detected in six iAMP21 cases and one dic(9;20) case with polysomy of chromosome 21. A fusion transcript joining exon 2 of RUNX1 with one of the first exons of DYRK1A could be confirmed in one of the cases (Supplementary Table 2). The samples with DYRK1A-RUNX1 fusion ($n = 6$) were amongst the samples with highest DYRK1A expression, however the difference did not reach statistical significance when compared with iAMP21 without fusion, and the expression level of RUNX1 did not differ significantly, neither between fusion positive and negative cases nor between iAMP21 and BCP ALL without iAMP21 (Supplementary Figure 3). There was no difference in median CN level between the groups. No RNA from the relapse was
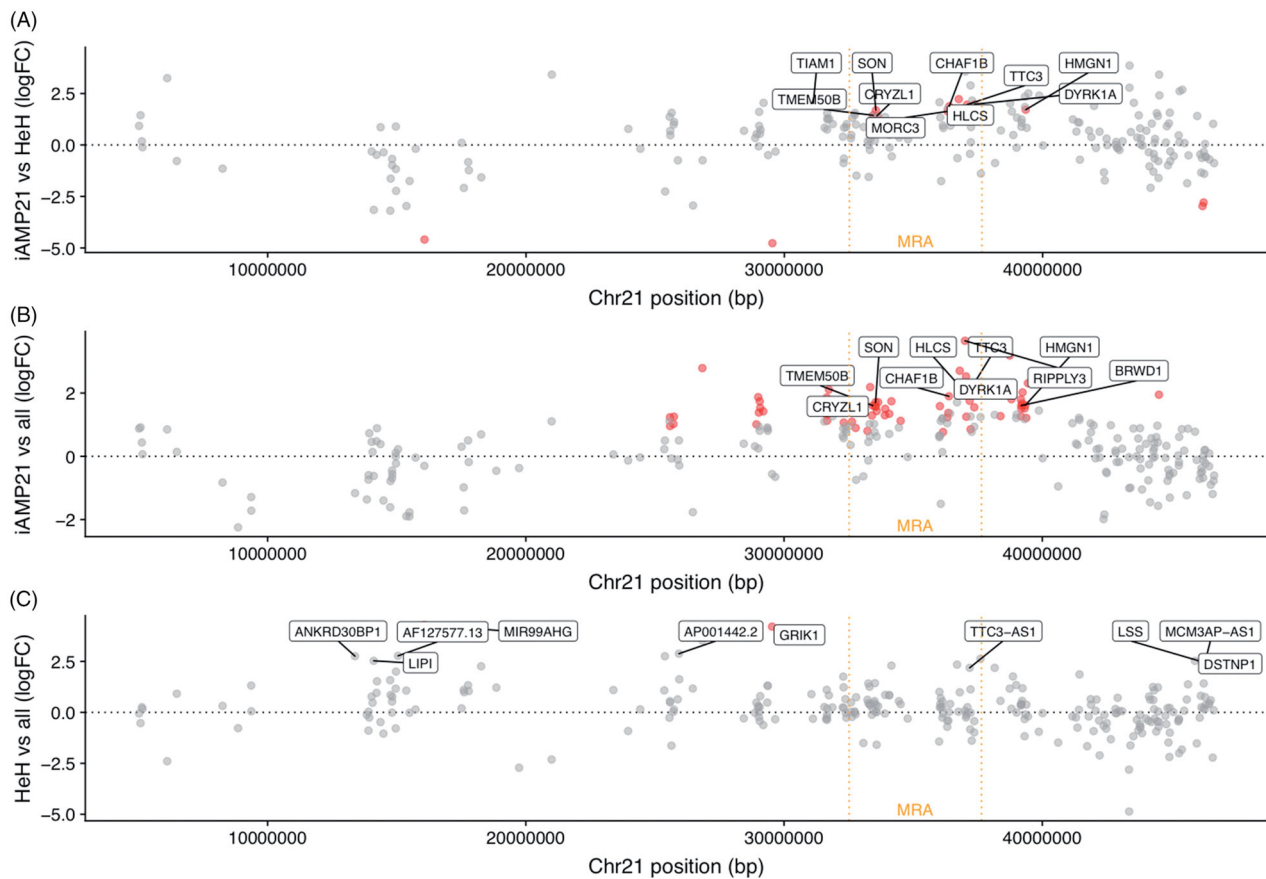
Figure 4. Graph showing expression level of genes throughout the chromosome 21q region in (A) iAMP21 vs. HeH, (B) iAMP21 vs. BCP ALL, and (C) HeH vs. BCP ALL. The top 10 overexpressed genes are denoted in each plot.

available for any of the diagnostic samples with the fusion.

Discussion

In this study, we used SNP array, WGS and RNA sequencing to investigate the genomic structure and the transcriptional profile of iAMP21-positive childhood BCP ALL, with the aim to understand the pathogenicity of the subtype. We could identify characteristic structural aberrations, i.e. terminal deletions and inverted end-fragments of chromosome 21q as well as oscillating CN states and multiple rearrangements, reflecting the mechanisms of formation proposed in previous studies [9–13,33]. Paired analysis of diagnostic and relapse sample showed different copy number states, suggesting that the rearrangement is unstable during the course of the disease. Mate-pair WGS showed individual rearrangement breakpoints on chromosome 21 in each case, with a low level of complexity in one of the cases, possibly reflecting differences in causative mechanisms within the iAMP21 group [13]. Furthermore, we detected the known iAMP21-associated CNAs outside of chromosome 21 [7,11,15]; deletions of the tumor

suppressor genes *SH2B3* and *RB1* were present in 40% of iAMP21 cases respectively, co-occurring in 25%. In agreement with a recent study reporting biallelic mutations and/or deletions of *SH2B3* in iAMP21 [16], a majority of the *SH2B3* deletions in our cohort were biallelic. Interestingly, this was also true for *RB1*; all deletions involving the 13q14 region were homozygous in a ~80 kb region spanning *RB1*, and while *SH2B3* RNA expression levels were unchanged in iAMP21 vs. BCP ALL without iAMP21, *RB1* was significantly underexpressed in iAMP21.

The differential expression profiling of iAMP21 vs. BCP ALL without iAMP21 showed, not surprisingly, that the top differentially expressed genes in iAMP21 were located on chromosome 21. In the MRA [11], two notable features were observed; first, over half of the amplified genes in this region (25/45) were not significantly overexpressed in iAMP21, and methylation analysis showed no pattern that could explain this variation. Second, the genes that were in fact overexpressed were among the genes with the highest and most consistent median expression in iAMP21; the top three were *DYRK1A*, *CHAF1B* and *SON*. An inverted fusion between *DYRK1A* and *RUNX1* was
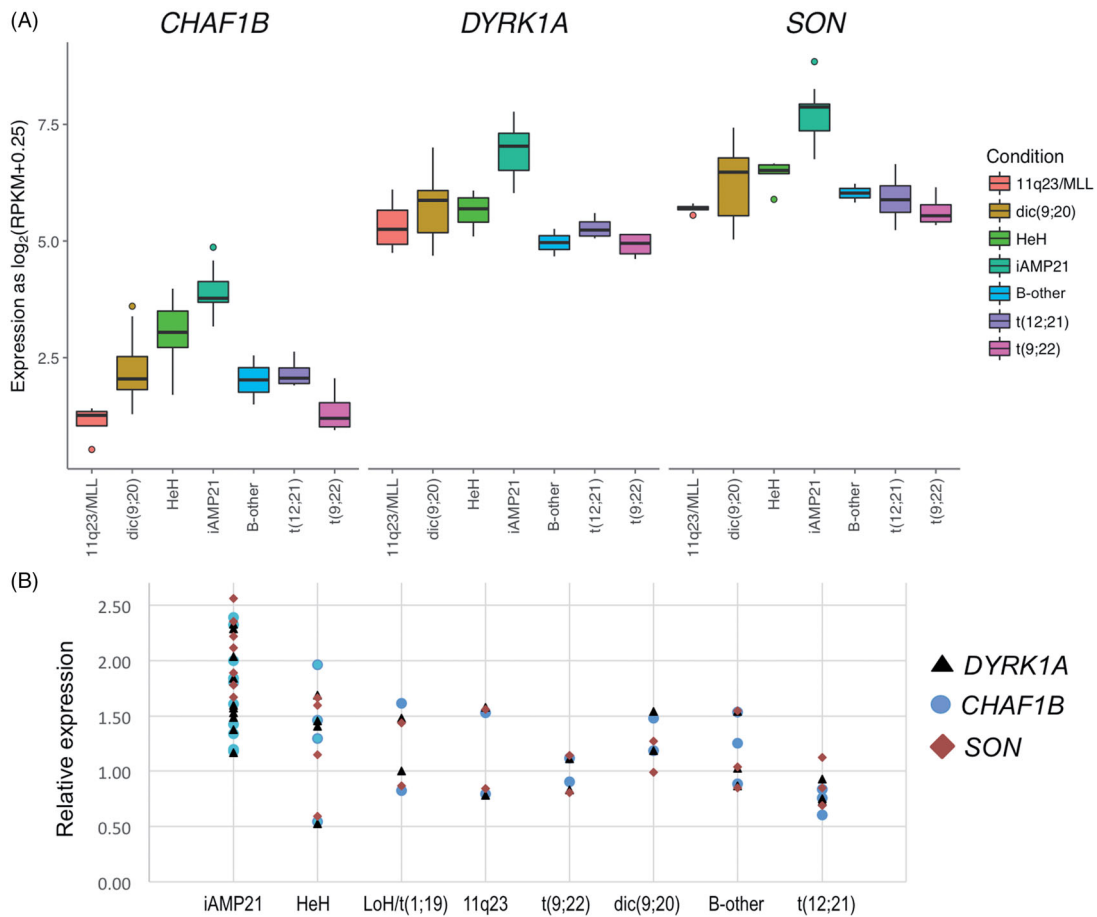
Figure 5. Expression of the top three most significantly overexpressed genes in the MRA in iAMP21 illustrated in (A) a box plot showing RNA sequencing results including mean expression levels in the different subtypes, and (B) a graph showing results from real-time RT-PCR for the different subtypes.

detected; a similar fusion has been reported previously [34], however, the fusion did not affect expression levels of *DYRK1A* or *RUNX1* and was not unique for iAMP21; the finding might be an effect of transcriptional read-through events enhanced by the high copy number state [35]. No other recurrent fusion genes were detected, and thus the pathogenicity of the subtype is likely not caused by oncogenic fusion genes.

Cases with HeH often harbor extra copies of chromosome 21 in their leukemic cells, and biological differences between these subtypes are likely relevant for the relapse tendency of iAMP21. Comparison of the two subtypes showed that the expression of chromosome 21 genes partly differs between the subtypes, and *DYRK1A, CHAF1B* and *SON* remained the top overexpressed genes in iAMP21 when compared with HeH only. A previous microarray expression study of iAMP21 could not demonstrate significant overexpression of these genes when compared with HeH [36]; the discrepancy is likely due to the different methods used. To further validate our results, we used

the RNA expression data from 376 BCP ALL cases in the St Jude's Pediatric Cancer Genome database (https://pecan.stjude.org) [37]; differential expression analysis showed significant overexpression of *DYRK1A* and *CHAF1B* in the iAMP21 group ($n = 15$) when compared to all BCP ALL cases ($p < 0.001$, Log fold change 1.6 and 1.5 respectively) but also when compared to HeH ($n = 13$) ($p < 0.001$ and $p = 0.01$, Log Fold Change 1.2 and 0.9 respectively) (Supplementary Figure 4), which further supports the relevance of our findings.

DYRK1A is a tyrosine kinase with both tumor suppressor and oncogenic features [38,39]. Fusions including *DYRK1A* have been described in ALL [40] and *DYRK1A* overexpression has been proposed as a tumor-promoting factor in Down syndrome (DS) ALL and acute megakaryocytic leukemia (AKML) [41–43] as well as in glioblastoma [44]. DYRK kinases are involved in lymphocyte differentiation and activation by several mechanisms, including phosphorylation of NFAT transcription factors and destabilization of cyclin D3, which promotes cell cycle exit and cell quiescence [45]. In gastrointestinal stromal tumors, DYRK1A

induces cell quiescence during treatment, thereby causing relapse [46]. Overexpression of *DYRK1A* could affect the balance between proliferation and differentiation in leukemic blast with iAMP21, and the quiescence promoting properties might be relevant for the relapse tendency. In a recent study on iAMP21, the authors hypothesized that *DYRK1A* might promote leukemia in cooperation with secondary abnormalities; however, the study did not include expression analysis to support their hypothesis [16].

CHAF1B encodes a major subunit of the chromatin assembly factor I, with critical functions for maintaining chromatin stability during DNA replication and repair [47]. Overexpression of *CHAF1B* has been associated with AKML in DS patients [43] and unfavorable prognosis in several malignancies [48–52]. In a recent study, overexpression of *CHAF1B* was shown to promote leukemogenesis by suppressing the expression of transcription factors in myeloid differentiation, including *FLI1*, *RUNX1* and *CEBPE* [53]. In our dataset, *FLI1* was significantly underexpressed, and *RUNX1* showed no change in expression despite amplification of the gene, possibly as an effect of *CHAF1B* overexpression. Further analysis of the expression of *FLI1* target genes [54] showed unchanged expression levels for the vast majority; only two genes, *HOxa10* and *RB1,* were underexpressed.

The *SON* gene encodes an RNA splicing factor with epigenetic functions affecting KMT2A complex assembly; short SON isoforms are upregulated in undifferentiated hematopoietic cells and leukemic blasts [55,56] and results in de-repression of KMT2A target genes [55]. Our RNA sequencing data could not differentiate between isoforms, however, DNA methylation analysis did not support that downstream SON targets were upregulated through hypomethylation in iAMP21.

In conclusion, this study has shown that the iAMP21 subtype has a heterogeneous genomic pattern but a unique transcriptional profile, with significant overexpression of biologically relevant genes in the amplified region on chromosome 21. We were able to identify three candidate genes, *DYRK1A*, *CHAF1B* and *SON*; each gene by its own right involved in malignant disease. *DYRK1A* and *CHAF1B* have expression level dependent functions [48–52,57] and all three genes are involved in chromatin remodeling, pointing to chromatin modification as a possible contributing mechanism for the pathogenicity in iAMP21. The tyrosine kinase and quiescence functions of DYRK1A, and the leukemogenic properties of *CHAF1B* overexpression indicate that these genes are particularly strong candidates. Further studies are needed to elucidate the functional role of these genes in the pathogenesis and treatment response of iAMP21-positive ALL.

Disclosure statement

No potential conflict of interest was reported by the authors.

ORCID

Ingegerd Ivanov Öfverholm http://orcid.org/0000-0002-6907-8004
Vasilios Zachariadis http://orcid.org/0000-0001-9360-9859
Fulya Taylan http://orcid.org/0000-0002-2907-0235
Yanara Marincevic-Zuniga http://orcid.org/0000-0001-5576-2115
Daniel Nilsson http://orcid.org/0000-0001-5831-385X
Magnus Nordenskjöld http://orcid.org/0000-0002-4974-425X
Ann Nordgren http://orcid.org/0000-0003-3285-4281
Jessica Nordlund http://orcid.org/0000-0001-8699-9959

References

[1] Schmiegelow K, Forestier E, Hellebostad M, et al. Long-term results of NOPHO ALL-92 and ALL-2000 studies of childhood acute lymphoblastic leukemia. Leukemia. 2010;24(2):345–354.

[2] Harewood L, Robinson H, Harris R, et al. Amplification of AML1 on a duplicated chromosome 21 in acute lymphoblastic leukemia: a study of 20 cases. Leukemia. 2003;17(3):547–553.

[3] Robinson HM, Broadfield ZJ, Cheung KL, et al. Amplification of AML1 in acute lymphoblastic leukemia is associated with a poor outcome. Leukemia. 2003;17(11):2249–2250.

[4] Moorman AV, Ensor HM, Richards SM, et al. Prognostic effect of chromosomal abnormalities in

childhood B-cell precursor acute lymphoblastic leukaemia: results from the UK Medical Research Council ALL97/99 randomised trial. Lancet Oncol. 2010;11(5): 429–438.

[5] Moorman AV, Robinson H, Schwab C, et al. Risk-directed treatment intensification significantly reduces the risk of relapse among children and adolescents with acute lymphoblastic leukemia and intrachromosomal amplification of chromosome 21: a comparison of the MRC ALL97/99 and UKALL2003 trials. JCO. 2013;31(27):3389–3396.

[6] Heerema NA, Carroll AJ, Devidas M, et al. Intrachromosomal amplification of chromosome 21 is associated with inferior outcomes in children with acute lymphoblastic leukemia treated in contemporary standard-risk children's oncology group studies: a report from the children's oncology group. JCO. 2013; 31(27):3397–3402.

[7] Harrison CJ, Moorman AV, Schwab C, et al. An international study of intrachromosomal amplification of chromosome 21 (iAMP21): cytogenetic characterization and outcome. Leukemia. 2014;28(5):1015–1021.

[8] Toft N, Birgens H, Abrahamsson J, et al. Results of NOPHO ALL2008 treatment for patients aged 1–45 years with acute lymphoblastic leukemia. Leukemia. 2018;32(3):606–615.

[9] Robinson HM, Harrison CJ, Moorman AV, et al. Intrachromosomal amplification of chromosome 21 (iAMP21) may arise from a breakage-fusion-bridge cycle. Genes Chromosom Cancer. 2007;46(4):318–326.

[10] Kuchinskaya E, Nordgren A, Heyman M, et al. Tiling-resolution array-CGH reveals the pattern of DNA copy number alterations in acute lymphoblastic leukemia with 21q amplification: the result of telomere dysfunction and breakage/fusion/breakage cycles? Leukemia. 2007;21(6):1327–1330.

[11] Rand V, Parker H, Russell LJ, et al. Genomic characterization implicates iAMP21 as a likely primary genetic event in childhood B-cell precursor acute lymphoblastic leukemia. Blood. 2011;117(25):6848–6855.

[12] Sinclair PB, Parker H, An Q, et al. Analysis of a breakpoint cluster reveals insight into the mechanism of intrachromosomal amplification in a lymphoid malignancy. Hum Mol Genet. 2011;20(13):2591–2602.

[13] Li Y, Schwab C, Ryan SL, et al. Constitutional and somatic rearrangement of chromosome 21 in acute lymphoblastic leukaemia. Nature. 2014;508(7494): 98–102.

[14] Baughn LB, Meredith MM, Oseth L, et al. SH2B3 aberrations enriched in iAMP21 B lymphoblastic leukemia. Cancer Genet. 2018;226–227:30–35.

[15] Ivanov Ofverholm I, Tran AN, Olsson L, et al. Detailed gene dose analysis reveals recurrent focal gene deletions in pediatric B-cell precursor acute lymphoblastic leukemia. Leuk Lymphoma. 2016;57:2161–2170.

[16] Sinclair PB, Ryan S, Bashton M, et al. SH2B3 inactivation through CN-LOH 12q is uniquely associated with B-cell precursor ALL with iAMP21 or other chromosome 21 gain. Leukemia 2019;33:1881–1894.

[17] Ryan SL, Matheson E, Grossmann V, et al. The role of the RAS pathway in iAMP21-ALL. Leukemia. 2016; 30(9):1824–1831.

[18] Nordlund J, Backlin CL, Wahlberg P, et al. Genome-wide signatures of differential DNA methylation in pediatric acute lymphoblastic leukemia. Genome Biol. 2013;14(9):r105.

[19] Marincevic-Zuniga Y, Dahlberg J, Nilsson S, et al. Transcriptome sequencing in pediatric acute lymphoblastic leukemia identifies fusion genes associated with distinct DNA methylation profiles. J Hematol Oncol. 2017;10(1):148.

[20] Venkatraman ES, Olshen AB. A faster circular binary segmentation algorithm for the analysis of array CGH data. Bioinformatics. 2007;23(6):657–663.

[21] Rasmussen M, Sundström M, Kultima H, et al. Allele-specific copy number analysis of tumor samples with aneuploidy and tumor heterogeneity. Genome Biol. 2011;12(10):R108.

[22] Neph S, Kuehn MS, Reynolds AP, et al. BEDOPS: high-performance genomic feature operations. Bioinformatics. 2012;28(14):1919–1920.

[23] Thorvaldsdottir H, Robinson JT, Mesirov JP. Integrative Genomics Viewer (IGV): high-performance genomics data visualization and exploration. Brief Bioinform. 2013;14(2):178–192.

[24] Tran AN, Taylan F, Zachariadis V, et al. High-resolution detection of chromosomal rearrangements in leukemias through mate pair whole genome sequencing. PLoS One. 2018;13(3):e0193928.

[25] Eisfeldt J, Vezzi F, Olason P, et al. TIDDIT, an efficient and comprehensive structural variant caller for massive parallel sequencing data. F1000Res. 2017;6:664.

[26] Dobin A, Davis CA, Schlesinger F, et al. STAR: ultrafast universal RNA-seq aligner. Bioinformatics. 2013;29(1): 15–21.

[27] Robinson MD, Oshlack A. A scaling normalization method for differential expression analysis of RNA-seq data. Genome Biol. 2010;11(3):R25.

[28] Law CW, Chen Y, Shi W, et al. Voom: precision weights unlock linear model analysis tools for RNA-seq read counts. Genome Biol. 2014;15(2):R29.

[29] Ritchie ME, Phipson B, Wu D, et al. Limma powers differential expression analyses for RNA-sequencing and microarray studies. Nucleic Acids Res. 2015;43(7):e47.

[30] Robinson JT, Thorvaldsdottir H, Winckler W, et al. Integrative genomics viewer. Nat Biotechnol. 2011; 29(1):24–26.

[31] Untergasser A, Nijveen H, Rao X, et al. Primer3Plus, an enhanced web interface to Primer3. Nucleic Acids Res. 2007;35(Web Server):W71–74.

[32] Nordlund J, Backlin CL, Zachariadis V, et al. DNA methylation-based subtype prediction for pediatric acute lymphoblastic leukemia. Clin Epigenet. 2015; 7(1):11.

[33] Bignell GR, Santarius T, Pole JC, et al. Architectures of somatic genomic rearrangement in human cancer amplicons at sequence-level resolution. Genome Res. 2007;17(9):1296–1303.

[34] Gu Z, Churchman M, Roberts K, et al. Genomic analyses identify recurrent MEF2D fusions in acute lymphoblastic leukaemia. Nat Commun. 2016;7(1):13331.

[35] Gingeras TR. Implications of chimaeric non-co-linear transcripts. Nature. 2009;461(7261):206–211.

[36] Strefford JC, van Delft FW, Robinson HM, et al. Complex genomic alterations and gene expression in acute lymphoblastic leukemia with intrachromosomal amplification of chromosome 21. Proc Natl Acad Sci U S A. 2006;103(21):8167–8172.

[37] Zhou X, Edmonson MN, Wilkinson MR, et al. Exploring genomic alteration in pediatric cancer using ProteinPaint. Nat Genet. 2016;48(1):4–6.

[38] Birger Y, Izraeli S. DYRK1A in down syndrome: an oncogene or tumor suppressor? J Clin Invest. 2012; 122(3):807–810.

[39] Abbassi R, Johns TG, Kassiou M, et al. DYRK1A in neurodegeneration and cancer: molecular basis and clinical implications. Pharmacol Ther. 2015;151:87–98.

[40] Roberts KG, Li Y, Payne-Turner D, et al. Targetable kinase-activating lesions in Ph-like acute lymphoblastic leukemia. N Engl J Med. 2014;371(11):1005–1015.

[41] Lee P, Bhansali R, Izraeli S, et al. The biology, pathogenesis and clinical aspects of acute lymphoblastic leukemia in children with Down syndrome. Leukemia. 2016;30(9):1816–1823.

[42] Letourneau A, Santoni FA, Bonilla X, et al. Domains of genome-wide gene expression dysregulation in Down's syndrome. Nature. 2014;508(7496):345–350.

[43] Malinge S, Bliss-Moreau M, Kirsammer G, et al. Increased dosage of the chromosome 21 ortholog Dyrk1a promotes megakaryoblastic leukemia in a murine model of Down syndrome. J Clin Invest. 2012; 122(3):948–962.

[44] Pozo N, Zahonero C, Fernandez P, et al. Inhibition of DYRK1A destabilizes EGFR and reduces EGFR-dependent glioblastoma growth. J Clin Invest. 2013;123(6): 2475–2487.

[45] Thompson BJ, Bhansali R, Diebold L, et al. DYRK1A controls the transition from proliferation to quiescence during lymphoid development by destabilizing Cyclin D3. J Exp Med. 2015;212(6):953–970.

[46] Boichuk S, Parry JA, Makielski KR, et al. The DREAM complex mediates GIST cell quiescence and is a novel therapeutic target to enhance imatinib-induced apoptosis. Cancer Res. 2013;73(16):5120–5129.

[47] Mjelle R, Hegre SA, Aas PA, et al. Cell cycle regulation of human DNA repair and chromatin remodeling genes. DNA Repair (Amst). 2015;30:53–67.

[48] de Tayrac M, Saikali S, Aubry M, et al. Prognostic significance of EDN/RB, HJURP, p60/CAF-1 and PDLI4, four new markers in high-grade gliomas. PLoS One. 2013;8(9):e73332.

[49] Staibano S, Mascolo M, Mancini FP, et al. Overexpression of chromatin assembly factor-1 (CAF-1) p60 is predictive of adverse behaviour of prostatic cancer. Histopathology. 2009;54(5):580–589.

[50] Staibano S, Mascolo M, Rocco A, et al. The proliferation marker Chromatin Assembly Factor-1 is of clinical value in predicting the biological behaviour of salivary gland tumours. Oncol Rep. 2011;25(1):13–22.

[51] Polo SE, Theocharis SE, Grandin L, et al. Clinical significance and prognostic value of chromatin assembly factor-1 overexpression in human solid tumours. Histopathology. 2010;57(5):716–724.

[52] Polo SE, Theocharis SE, Klijanienko J, et al. Chromatin assembly factor-1, a marker of clinical value to distinguish quiescent from proliferating cells. Cancer Res. 2004;64(7):2371–2381.

[53] Volk A, Liang K, Suraneni P, et al. A CHAF1B-dependent molecular switch in hematopoiesis and leukemia pathogenesis. Cancer Cell. 2018;34(5):707.e7–723.e7.

[54] Li Y, Luo H, Liu T, et al. The ets transcription factor Fli-1 in development, cancer and disease. Oncogene. 2015;34(16):2022–2031.

[55] Kim JH, Baddoo MC, Park EY, et al. SON and Its alternatively spliced isoforms control MLL complex-mediated H3K4me3 and transcription of leukemia-associated genes. Mol Cell. 2016;61(6):859–873.

[56] Ahn EE, Higashi T, Yan M, et al. SON protein regulates GATA-2 through transcriptional control of the microRNA 23a∼27a∼24-2 cluster. J Biol Chem. 2013; 288(8):5381–5388.

[57] Aranda S, Laguna A, de la Luna S. DYRK family of protein kinases: evolutionary relationships, biochemical properties, and functional roles. FASEB J. 2011;25(2): 449–462.